Local Coordinate Systems-Based Method to Analyze High-order Modes of *n*-Step Timoshenko Beam

M.S. Cao[1], W. Xu[1,*], N. Xia[1], Z. Su[2], S.S. Wang[1]

[1]Department of Engineering Mechanics, Hohai University, Nanjing 210098, China

[2]Department of Mechanical Engineering, The Hong Kong Polytechnic University, Hung Hom, Kowloon, Hong Kong Special Administrative Region, Hong Kong

[*]Corresponding author, E-mail: xuwei2007hohai@hhu.edu.cn

Abstract: High-frequency transverse vibration of stepped beams has attracted increasing attention in various industrial areas. For an *n*-step Timoshenko beam, the governing differential equations of transverse vibration have been well established based on assembling classical Timoshenko's beam equations for uniform beam segments in the literature. However, solving the governing differential equation has not resolved well to date, manifested by a computational bottleneck: only first *k* modes ($k \leqslant 12$) are solvable for *i*-step ($i \geqslant 0$) Timoshenko beams. This bottleneck influences the completeness of the stepped Timoshenko beam theory. To address this problem, this study first reveals the root cause for the bottleneck in solving the governing differential equations for high-order modes, and then creates a sophisticated local coordinate systems-based method that can overcome the bottleneck to accomplish high-order mode shapes of an *n*-step Timoshenko beam. The proposed method uses a set of local coordinate systems in place of the conventional global coordinate system to characterize the transverse vibration of a *n*-step Timoshenko beam. With the method, these local coordinate systems can simplify the frequency equation for the *n*-step Timoshenko beam's vibration, making it possible to obtain high-order modes of the beam. The accuracy, capacity, and efficiency of the local coordinate systems-based method in acquiring high-order modes are corroborated using the well-known exact dynamic stiffness method underpinned by the Wittrick-Williams algorithm as a reference. The removal of the bottlenecks in solving the governing differential equations for high-order modes usefully contributes to the completeness of the stepped Timoshenko beam theory.

Keywords: stepped Timoshenko beam; high-order mode; governing differential equation; modal frequency; mode shape; local coordinate system; exact dynamic stiffness; Wittrick-Williams algorithm

1 Introduction

Timoshenko beam theory is a classical engineering beam theory that is superior to Euler-Bernoulli beam theory in portraying shear deformation and rotary inertia (Timoshenko, 1922; Han et al., 1999; Majkut, 2009). The inclusion of shear deformation and rotary inertia renders that Timoshenko beam theory provides a theoretical basis for characterizing high-frequency transverse vibration (besides low-frequency transverse vibration) of beams, where the shear deformation and rotary inertia are significant and should be considered in vibration analysis. A generalized version of a Timoshenko beam is a stepped Timoshenko beam that consists of a group of uniform beam segments joined at the cross-section step. A stepped Timoshenko beam with carefully arranged material and/or geometrical properties for each beam segment is able to represent a uniform beam, a beam of gradually changed cross-sections, a cracked beam, and their combinations (Failla, 2011; Park and Stallings, 2003; Park and Stallings, 2005).

Although the low-frequency transverse vibration of a stepped Timoshenko beam has been extensively investigated by various approaches, the high-frequency transverse vibration is still an active research focus due to more complexity and challenges (Hsu et al., 2007; Wu and Thompson, 1999). The core of high-frequency transverse vibration analysis is the high-order modal analysis, from which the superposition of high-order modes forms the transverse vibration responses. In existing work, the high-order modes of a stepped Timoshenko beam are primarily studied by three categories of methods: finite element (FE) method, exact dynamic stiffness (EDS) scheme, and governing equation-solving (GES) method. The basic functionality of these methods to analyze high-order modes of a stepped Timoshenko beam are briefed as follows.

FE method: the FE method uses frequency-independent polynomial shape functions to simulate the vibration deformation of discrete elements jointed at nodes (Kapur, 1966; Dawe,

1978). To characterize the high-order modes, the refinement of FE meshes is required to make the polynomial shape function reasonably approximate the element deformation. In essence, the polynomial shape functions cannot exactly portray the complex shape of high-order modes, so the FE method can only provide approximate solutions to the high-order modes. Moreover, use of the FE method to obtain high-order modes is seriously hindered by the huge computation cost when extremely fine FE meshes are needed to describe the intricate shape of high-order modes (Wei et al., 2002). Therefore, it is generally acknowledged that the FE method is not an efficient tool to obtain high-order modes of a stepped Timoshenko beam.

EDS scheme: the EDS method underpinned by the sophisticated Wittrick-Williams (W-W) algorithm (Williams and Wittrick, 1970; Wittrick and Williams, 1971; Williams and Wittrick, 1983; Williams and Kennedy, 2010) functions as a robust scheme to obtain solutions of high-order modes of discontinuous or stepped Timoshenko beams (Howson and Williams, 1973; Pilkey and Kitis, 1994; Banerjee and Williams, 1996; Banerjee, 1997; Banerjee, 2001; Banerjee, 2003; Yuan et al., 2007; Li et al., 2008; Yu and Roesset, 2011; Greco and Pau, 2012): (i) With the EDS method, the EDS matrix of a beam member is formulated using frequency-dependent exact dynamic shape functions derived from general wave solutions of the Timoshenko's beam equations for the beam member. As the exact dynamic shape functions can readily capture all necessary high-frequency wave modes of interest, extremely highly accurate solutions can be characterized with no need for refined meshes for a beam member (Howson and Williams, 1973; Yuan et al., 2007). The EDS matrices of beam members are assembled to form the global EDS matrix for the stepped beam. (ii) With the W-W algorithm, the global EDS matrix is processed by counting the number of modal frequencies exceeded by a given frequency, rather than directly calculating modal frequencies from the global EDS matrix, to give modal frequencies (Williams and Wittrick, 1970; Wittrick and Williams, 1971; Williams and Wittrick, 1983; Williams and Kennedy, 2010; Howson and Williams, 1973;

Pilkey and Kitis, 1994; Banerjee and Williams, 1996; Banerjee, 1997; Banerjee, 2001; Banerjee, 2003; Yuan et al., 2007; Li et al., 2008; Yu and Roesset, 2011; Greco and Pau, 2012). In principle, the EDS method involves some similar steps to those of the FE method: formation of element stiffness matrix, assembly to form global stiffness matrix, introduction of boundary conditions, evaluation of nodes' displacement variables, etc. However, the EDS method has a distinct feature from the conventional FE method: it uses frequency-dependent exact dynamic shape functions to arrive at the solutions of high-order modes, with no need for solving the governing differential equations of a stepped Timoshenko beam.

GES method: the GES method solves the governing differential equations of a stepped Timoshenko beam to acquire its high-order modes. Solving Timoshenko beam equations has been an active research topic after the proposition of the equations by Timoshenko (Timoshenko, 1922; Huang, 1961). The governing differential equation for a stepped Timoshenko beam has widely appeared in the literature (Tong et al., 1995; Dong et al., 2005; Zhang et al., 2014): it comprises a group of differential equations for uniform beam segments along with continuity conditions at the cross-section steps and boundary conditions at the ends (Dong et al., 2005). Up to date, GES methods to obtain low-order modes for stepped beams, typically stepped Timoshenko beams, have been investigated in various studies (Tong et al., 1995; Dong et al., 2005; Zhang et al., 2014; Ju et al., 1994; Lee and Ng, 1994; Lu et al., 2009; Lee et al., 2009; Gupta and Sharma, 1998; Suddoung, 2013; Kisa and Arif Gurel, 2007; Naguleswaran, 2002); however, GES methods to attain high-order modes of a stepped Timoshenko beam has not been resolved well (Wu and Thompson, 1999; Kapur, 1996; Yuan et al., 2007).

The difficulties in solving the governing differential equations of a stepped Timoshenko beam to obtain its high-order modes are described as follows. The frequency equation of an *n*-step Timoshenko beam commonly contains numerous multiplied hyperbolic functions

$\sinh a_k$ and/or $\cosh a_k$ (Horr, 1995), such that it can be only tackled by the digital computer-aided methods (Low, 1993). Unfortunately, existing digital computer-aided methods allow determination of only a small quantity of low-order modes from the frequency equation (Low, 1993; Tang, 2003; Goncalves, 2007; Xu et al., 2014), within the capacity of digital computer. When high-order modes are attacked, an unexpected computational error occurs as a result of the immense value present in evaluation of the frequency equation, exceeding the limit capacity of digital computers (Tang, 2003; Goncalves, 2007; Xu et al., 2014), leaving a computational bottleneck for high-order modes of a stepped Timoshenko beam.

This computational bottleneck appears as a common instance when solving the governing differential equations containing hyperbolic functions for an arbitrary beam (Low, 1993; Tang, 2003; Goncalves, 2007; Xu et al., 2014). By way of illustration, the loosest computational bottleneck for a zero-step (uniform) Timoshenko beam is exhibited in Figure 1. Figure 1(a) presents the profile of frequency determinant $D(\omega)$ versus frequency ω, of which valid zero-crossings specify the modal frequency ω_i. Clearly, the modal frequencies up to ω_{12} can be determined from the profile, but the higher-order modal frequencies cannot be identified due to the abnormality of the profile over that frequency scope. To gain a better insight into this occurrence, modal analysis is performed with the given results (Figure 1(b)): the 11th mode shape runs stably and normally, but the 12th mode shape behaves a little irregularly in the vicinity of $\zeta = 0$ and $\zeta = 1$, as labeled by the ellipses, where ζ is the dimensionless coordinate of beam length. This instance specifies the 12th-mode bottleneck for a zero-step Timoshenko beam. In common, kth-mode (k<12) bottlenecks exist for i-step (i>0) Timoshenko beams.

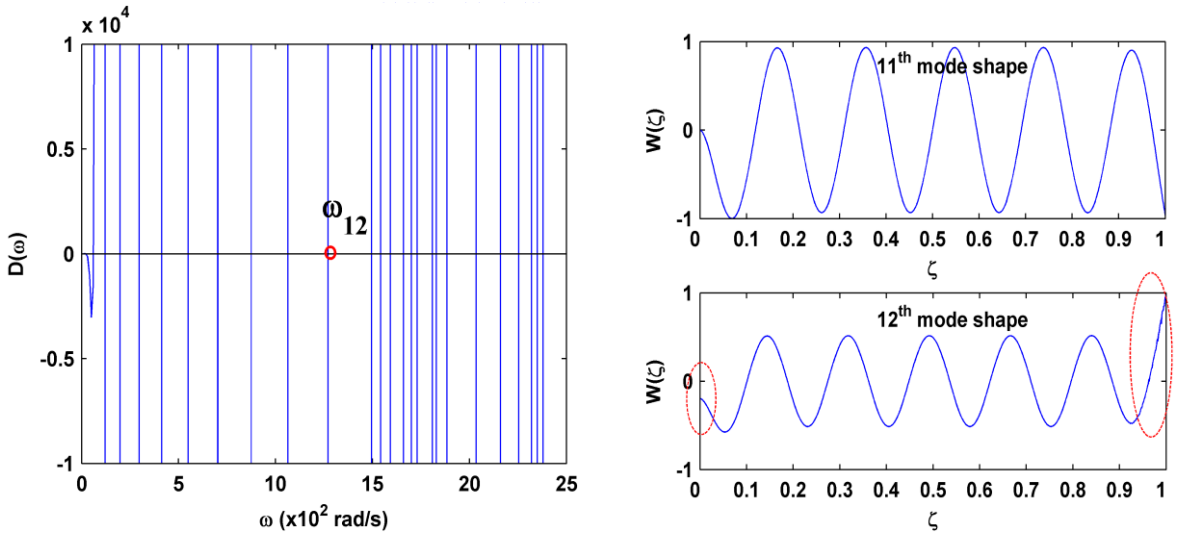

(a) (b)

Figure 1. 12th-mode bottleneck in acquisition of high-order modes by solving zero-step (uniform) Timoshenko beam frequency equation. (a) Profile of frequency determinant versus frequency; (b) 11th and 12th mode shapes.

To address the computational bottleneck, this study creates a new method for solving the governing differential equations of a stepped Timoshenko beam to yield its high-order modes. This method is formulated using a set of local coordinate systems (LCSs) in place of the conventional single global coordinate system (GCS) to reformat the governing differential equations of a stepped Timoshenko beam. The frequency equation derived from the reformatted governing differential equations is significantly simplified such that it allows determination of high-order modes. The accuracy, capacity, and efficiency of the proposed methods are sufficiently corroborated by the EDS scheme with the W-W algorithm capturing modal frequencies reliably (Williams and Wittrick, 1970; Wittrick and Williams, 1971; Williams and Wittrick, 1983; Williams and Wittrick, 1983; Williams and Kennedy, 2010; Howson and Williams, 1973; Pilkey and Kitis, 1994; Banerjee and Williams, 1996; Banerjee, 1997; Banerjee, 2001; Banerjee, 2003; Yuan et al., 2007; Li et al., 2008; Yu and Roesset, 2011; Greco and Pau, 2012).

2 Problem formulation

2.1 Transverse vibration model

The basic procedure for building a transverse vibration model of an *n*-step Timoshenko beam (Tong et al., 1995) is illustrated on a two-step cantilever beam with the *i*th step in the cross-section identified by the distance L_i, $i=1-3$, from the clamped end in a GCS of the origin at the clamped end (Figure 2). Using Timoshenko beam theory (Timoshenko, 1922), the governing differential equations for free flexural transverse vibration of each segment are expressed as

$$E_i I_i \frac{\partial^2 \varphi_i(x,t)}{\partial x^2} + k_i G_i A_i \left(\frac{\partial w_i(x,t)}{\partial x} - \varphi_i(x,t) \right) - \rho_i I_i \frac{\partial^2 \varphi_i(x,t)}{\partial t^2} = 0, \tag{1.1}$$

$$k_i G_i \left(\frac{\partial^2 w_i(x,t)}{\partial x^2} - \frac{\partial \varphi_i(x,t)}{\partial x} \right) - \rho_i \frac{\partial^2 w_i(x,t)}{\partial t^2} = 0, \tag{1.2}$$

where $w_i(x,t)$ is the transverse deflection, $\varphi_i(x,t)$ the rotational angle due to bending, E_i the modulus of elasticity, G_i the shear modulus, I_i the area moment of inertia, ρ_i the mass density of the material, A_i the cross-sectional area, and κ_i the shear coefficient for the cross-section.

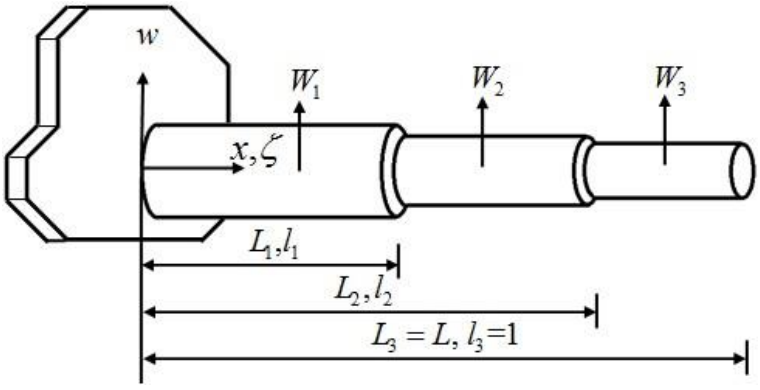

Figure 2. Two-step cantilever beam in GCS.

We assume that solutions of equations (1.1) and (1.2) consist of spatial and temporal parts expressed as

$$w_i(x,t) = R_i(x)e^{j\omega t}, \quad \varphi_i(x,t) = \psi_i(x)e^{j\omega t}, \tag{2}$$

where R_i and ψ_i are spatial variables, i.e., the amplitudes of transverse deflection and rotational angle, respectively, and ω is the circular frequency. Substitution of equation (2) into equation (1), together with employment of the coordinate variables:

$$\zeta = \frac{x}{L}, \quad W_i = \frac{R_i}{L}, \quad \varsigma = \frac{t}{\sqrt{L}};$$

and geometrical and material variables:

$$l_i = \frac{L_i}{L}, \quad \vartheta_i = \frac{E_i}{k_i G_i}, \quad r_i = \frac{1}{A_i L^2}, \quad s_i = \vartheta_i r_i, \quad \tau_i = \frac{\rho_i A_i}{E_i I_i} L^4 \omega^2, \quad \alpha_i = \frac{\tau_i (r_i + s_i)}{2}, \quad \beta_i = \tau_i (\tau_i r_i s_i - 1),$$

yields the coupled equations with respect to W_i and ψ_i (Huang, 1961):

$$\frac{d^4}{d\zeta^4} W_i(\zeta) + 2\alpha_i \frac{d^2}{d\zeta^2} W_i(\zeta) + \beta_i W_i(\zeta) = 0, \tag{3.1}$$

$$\frac{d^4}{d\zeta^4} \psi_i(\zeta) + 2\alpha_i \frac{d^2}{d\zeta^2} \psi_i(\zeta) + \beta_i \psi_i(\zeta) = 0. \tag{3.2}$$

Let $\gamma_{i,1} = (\sqrt{\alpha_i^2 - \beta_i} - \alpha_i)^{1/2}$, $\gamma_{i,2} = (\sqrt{\alpha_i^2 - \beta_i} + \alpha_i)^{1/2}$, $m_{i,1} = \frac{\tau_i s_i + \gamma_{i,1}^2}{\gamma_{i,1}}$, $m_{i,2} = \frac{\tau_i s_i - \gamma_{i,2}^2}{\gamma_{i,2}}$ and the general solutions for W_i and ψ_i are (Lin, 2004; Khaji et al., 2009; Caliò and Greco, 2012)

$$W_i(\zeta) = A_i \cosh \gamma_{i,1}\zeta + B_i \sinh \gamma_{i,1}\zeta + C_i \cos \gamma_{i,2}\zeta + D_i \sin \gamma_{i,2}\zeta, \quad l_{i-1} \le \zeta \le l_i, \tag{4.1}$$

$$\psi_i(\zeta) = A_i m_{i,1} \sinh \gamma_{i,1}\zeta + B_i m_{i,1} \cosh \gamma_{i,1}\zeta + C_i m_{i,2} \sin \gamma_{i,2}\zeta - D_i m_{i,2} \cos \gamma_{i,2}\zeta, \quad l_{i-1} \le \zeta \le l_i, \tag{4.2}$$

with their derivatives $W_i'(\zeta)$ and $\psi_i'(\zeta)$:

$$W_i'(\zeta) = A_i \gamma_{i,1} \sinh \gamma_{i,1}\zeta + B_i \gamma_{i,1} \cosh \gamma_{i,1}\zeta - C_i \gamma_{i,2} \sin \gamma_{i,2}\zeta + D_i \gamma_{i,2} \cos \gamma_{i,2}\zeta, \quad l_{i-1} \le \zeta \le l_i, \tag{4.3}$$

$$\boldsymbol{\psi}_i'(\zeta) = A_i m_{i,1} \gamma_{i,1} \cosh \gamma_{i,1}\zeta + B_i m_{i,1} \gamma_{i,1} \sinh \gamma_{i,1}\zeta + C_i m_{i,2} \gamma_{i,2} \cos \gamma_{i,2}\zeta + D_i m_{i,2} \gamma_{i,2} \sin \gamma_{i,2}\zeta, \quad l_{i-1} \le \zeta \le l_i, \tag{4.4}$$

In equations (3) and (4), $A_i - D_i$, $i = 1,2,3$ are arbitrary constants to be determined by the continuity conditions at the steps of cross-section and boundary conditions at the beam ends. The continuity conditions at $\zeta = l_1$ are

$$W_1(\zeta)=W_2(\zeta)\big|_{\zeta=l_1},\qquad W_1^{'}(\zeta)=W_2^{'}(\zeta)\big|_{\zeta=l_1},$$
$$E_1I_1\psi_1^{'}(\zeta)=E_2I_2\psi_2^{'}(\zeta)\big|_{\zeta=l_1},\ \ k_1G_1A_1(W_1^{'}(\zeta)-\psi_1(\zeta))=k_2G_2A_2(W_2^{'}(\zeta)-\psi_2(\zeta))\big|_{\zeta=l_1}, \tag{5.1}$$

and those at $\zeta=l_2$ are

$$W_2(\zeta)=W_3(\zeta)\big|_{\zeta=l_2},\qquad W_2^{'}(\zeta)=W_3^{'}(\zeta)\big|_{\zeta=l_2},$$
$$E_2I_2\psi_2^{'}(\zeta)=E_2I_3\psi_3^{'}(\zeta)\big|_{\zeta=l_2},\ \ k_2G_2A_2(W_2^{'}(\zeta)-\psi_2(\zeta))=k_3G_3A_3(W_3^{'}(\zeta)-\psi_3(\zeta))\big|_{\zeta=l_2}. \tag{5.2}$$

The boundary conditions at $\zeta=0$ and $\zeta=1$ are specified by

$$W_1(\zeta)\big|_{\zeta=0}=0,\ \ \psi_1(\zeta)\big|_{\zeta=0}=0,\ \ \psi_2^{'}(\zeta)\big|_{\zeta=1}=0,\ \ (W_2^{'}(\zeta)-\psi_2(\zeta))\big|_{\zeta=1}=0. \tag{5.3}$$

Substituting equation (4) into equation (5), we obtain a group of simultaneous equations:

$$\mathbf{D}(\omega)\mathbf{C}=0, \tag{6}$$

where $\mathbf{C}$ is a coefficient vector of A_i-D_i, i=1-3, and $\mathbf{D}(\omega)$ is the characteristic matrix (12×12) with its entries containing the unknown ω. The frequency determinant $D(\omega)$ associated with the characteristic matrix is

$$D(\omega)=\begin{vmatrix} O_{1(2\times4)} & 0_{(2\times4)} & 0_{(2\times4)} \\ P_{1(4\times4)} & Q_{1(4\times4)} & 0_{(4\times4)} \\ 0_{(4\times4)} & P_{2(4\times4)} & Q_{2(4\times4)} \\ 0_{(2\times4)} & 0_{(2\times4)} & O_{2(2\times4)} \end{vmatrix}. \tag{7}$$

with sub-blocks O_1, O_2, P_1, P_2, Q_1, and Q_2 detailed by

$$O_1=\begin{pmatrix} 1 & 0 & 1 & 0 \\ 0 & m_{1,1} & 0 & -m_{1,2} \end{pmatrix},$$

$$P_1=\begin{pmatrix} \cosh a_1 & \sinh a_1 & \cos a_2 & \sin a_2 \\ \gamma_{1,1}\sinh a_1 & \gamma_{1,1}\cosh a_1 & -\gamma_{1,2}\sin a_2 & \gamma_{1,2}\cos a_2 \\ m_{1,1}\gamma_{1,1}\cosh a_1 & m_{1,1}\gamma_{1,1}\sinh a_1 & m_{1,2}\gamma_{1,2}\cos a_2 & m_{1,2}\gamma_{1,2}\sin a_2 \\ (\gamma_{1,1}-m_{1,1})\sinh a_1 & (\gamma_{1,1}-m_{1,1})\cosh a_1 & -(\gamma_{1,2}+m_{1,2})\sin a_2 & (\gamma_{1,2}+m_{1,2})\cos a_2 \end{pmatrix},$$

$$Q_1=\begin{pmatrix} -\cosh a_3 & -\sinh a_3 & -\cos a_4 & -\sin a_4 \\ -\gamma_{2,1}\sinh a_3 & -\gamma_{2,1}\cosh a_3 & \gamma_{2,2}\sin a_4 & -\gamma_{2,2}\cos a_4 \\ -F_1 m_{2,1}\gamma_{2,1}\cosh a_3 & -F_1 m_{2,1}\gamma_{2,1}\sinh a_3 & -F_1 m_{2,2}\gamma_{2,2}\cos a_4 & -F_1 m_{2,2}\gamma_{2,2}\sin a_4 \\ -K_1(\gamma_{2,1}-m_{2,1})\sinh a_3 & -K_1(\gamma_{2,1}-m_{2,1})\cosh a_3 & K_1(\gamma_{2,2}+m_{2,2})\sin a_4 & -K_1(\gamma_{2,2}+m_{2,2})\cos a_4 \end{pmatrix},$$

$$P_2=\begin{pmatrix} \cosh a_5 & \sinh a_5 & \cos a_6 & \sin a_6 \\ \gamma_{2,1}\sinh a_5 & \gamma_{2,1}\cosh a_5 & -\gamma_{2,2}\sin a_6 & \gamma_{2,2}\cos a_6 \\ m_{2,1}\gamma_{2,1}\cosh a_5 & m_{2,1}\gamma_{2,1}\sinh a_5 & m_{2,2}\gamma_{2,2}\cos a_6 & m_{2,2}\gamma_{2,2}\sin a_6 \\ (\gamma_{2,1}-m_{2,1})\sinh a_5 & (\gamma_{2,1}-m_{2,1})\cosh a_5 & -(\gamma_{2,2}+m_{2,2})\sin a_6 & (\gamma_{2,2}+m_{2,2})\cos a_6 \end{pmatrix},$$

$$Q_2=\begin{pmatrix} -\cosh a_7 & -\sinh a_7 & -\cos a_8 & -\sin a_8 \\ -\gamma_{3,1}\sinh a_7 & -\gamma_{3,1}\cosh a_7 & \gamma_{3,2}\sin a_8 & -\gamma_{3,2}\cos a_8 \\ -F_2 m_{3,1}\gamma_{3,1}\cosh a_7 & -F_2 m_{3,1}\gamma_{3,1}\sinh a_7 & -F_2 m_{3,2}\gamma_{3,2}\cos a_8 & -F_2 m_{3,2}\gamma_{3,2}\sin a_8 \\ -K_2(\gamma_{3,1}-m_{3,1})\sinh a_7 & -K_2(\gamma_{3,1}-m_{3,1})\cosh a_7 & K_2(\gamma_{3,2}+m_{3,2})\sin a_8 & -K_2(\gamma_{3,2}+m_{3,2})\cos a_8 \end{pmatrix},$$

$$O_2=\begin{pmatrix} m_{3,1}\gamma_{3,1}\cosh a_9 & m_{3,1}\gamma_{3,1}\sinh a_9 & m_{3,2}\gamma_{3,2}\cos a_{10} & m_{3,1}\gamma_{3,2}\sin a_{10} \\ (\gamma_{3,1}-m_{3,1})\sinh a_9 & (\gamma_{3,1}-m_{3,1})\cosh a_9 & -(\gamma_{3,2}+m_{3,2})\sin a_{10} & (\gamma_{3,2}+m_{3,2})\cos a_{10} \end{pmatrix},$$

where

$$\begin{aligned} &a_1=\gamma_{1,1}l_1,\ \ a_2=\gamma_{1,2}l_1,\ \ a_3=\gamma_{2,1}l_1,\ \ a_4=\gamma_{2,2}l_1,\ \ a_5=\gamma_{2,1}l_2, \\ &a_6=\gamma_{2,2}l_2,\ \ a_7=\gamma_{3,1}l_2,\ \ a_8=\gamma_{3,2}l_2,\ \ a_9=\gamma_{3,1}l_3,\ \ a_{10}=\gamma_{3,2}l_3, \end{aligned} \tag{8}$$

and

$$F_1=\frac{E_2I_2}{E_1I_1},\ \ K_1=\frac{k_2G_2A_2}{k_1G_1A_1},\ \ F_2=\frac{E_3I_3}{E_2I_2},\ \ K_2=\frac{k_3G_3A_3}{k_2G_2A_2}. \tag{9}$$

In $D(\omega)$, the sub-blocks O_1 and O_2 group the elements related to the boundary conditions at ends $\zeta=0$ and $\zeta=l_3$; the sub-blocks P_1 and Q_1 group the elements related to the continuity conditions at the first step of cross-section $\zeta=l_1$; the sub-blocks P_2 and Q_2 group the elements related to the continuity conditions at the second step of cross-section $\zeta=l_2$, respectively.

Setting the frequency determinant $D(\omega)$ to zero yields the frequency equation:

$$D(\omega)=0. \tag{10}$$

Ideally, solving equation (10) can produce a series of modal frequencies ω_j. Provided with ω_j, the coefficient vector $\mathbf{C}$ in equation (6) can be solved. Substitution of ω_j and $\mathbf{C}$ into equations (4.1) yields the mode shape W_i^j. Unfortunately, it is extremely intractable to solve equation (10) due to its tremendous complexity.

2.2 Problem description

The frequency equation $D(\omega)=0$ is a higher-order transcendental function with a large number of terms, each containing multiple multiplied hyperbolic functions $\sinh a_k$ and/or $\cosh a_k$ (Low, 1993). This feature makes analytical solution of the frequency equation intractable, so that digital computer-aided methods are required to tackle the equation. Among available digital computer-aided methods, the direct determinant evaluation (DDE) method is most promising due to its flexibility (Low, 1993). The basics of the DDE method are: at a given value of ω, evaluate every entry of $D(\omega)$, in turn yielding the estimate of $D(\omega)$ using algebraic operation of entries. Provided with a sequence of ω, a profile of $D(\omega)$ versus ω can be produced, of which the zero-crossings specify the solutions of $D(\omega)=0$.

However, when we use the DDE method to deal with the frequency equation $D(\omega)=0$, the resultant profile of $D(\omega)$ versus ω exhibits some abnormalities when ω exceeds a certain value, as illustrated in Figure 3 for Model I with the geometrical and material parameters listed in Table 1 and Table 2, respectively. Figure 3(a) shows the profile of $Y(\omega)$ versus ω as an alternative profile of $D(\omega)$ versus ω for clear presentation of frequency scope (0,1000) rad/s. The relation between $D(\omega)$ and $Y(\omega)$ is given as

$$Y(\omega)=\sinh^{-1}(D(\omega))=\ln(D(\omega)+\sqrt{D(\omega)^2+1}). \tag{11}$$

Table 1. Geometrical parameters of stepped Timoshenko beam models

Model	Length (L_i [m])	Cross-section area (A_i [10^{-4} m^2])	Moment of inertia (I_i [8.33×10^{-10} m^4])
I	0.4, 0.3, 0.3	1, 1.21, 1	1, 1.331, 1
II	0.25, 0.3, 0.4, 0.25	1, 1.44, 1, 1	1, 1.728, 1, 1
III	0.2, 0.3, 0.2, 0.25, 0.3	1, 1.21, 1, 1.44, 1	1, 1.331, 1, 1.728, 1
IV	0.3, 0.2, 0.3, 0.4, 0.3, 0.2	1, 1.44, 1, 1.21, 1, 1.44	1, 1.728, 1, 1.31, 1, 1.728
V	0.2, 0.2, 0.3, 0.3	1, 1, 1.21, 1	1, 1, 1.331, 1

Table 2. Material parameters of stepped Timoshenko beam models

Model	Elastic modulus (E_i [10^9 $Kgm^{-1}s^{-2}$])	Shear modulus (G_i [$3.8\times10^8 Kgm^{-1}s^{-2}$])	Density (ρ_i [10^4 Kgm^{-3}])	Shear coefficient (k_i)
I	1, 0.8, 0.6	1, 0.8, 0.6	1, 0.7, 0.5	0.8864
II	0.5, 0.6, 0.4, 0.3	0.5, 0.6, 0.4, 0.3	0.8, 0.7, 0.7, 0.8	0.8864
III	0.6, 0.8, 0.6, 0.8, 0.6	0.6, 0.8, 0.6, 0.8, 0.6	0.5, 0.8, 0.7, 0.6, 0.8	0.8864
IV	07, 0.6, 0.7, 0.6, 0.7, 0.6	07, 0.6, 0.7, 0.6, 0.7, 0.6	0.8, 0.7, 0.8, 0.7, 0.6, 0.7	0.8864
V	1, 1, 0.8, 0.6	1, 1, 0.8, 0.6	1, 1, 0.7, 0.5	0.8864

In Figure 3(a), the portion of the profile over the frequency interval [0, 535] rad/s behaves stably and regularly, from which the modal frequencies up to ω_8 can be basically determined, whereas the portion going beyond the frequency 535 rad/s acts erratically and irregularly, delivering no any information as to modal frequency. To provide a better insight into this phenomenon, the critical 7^{th} and 8^{th} mode shapes are explored (Figure 3(b)) with the yielded results: the 7^{th} mode shape runs stably and normally, whereas the 8^{th} mode shape behaves a little irregularly in the vicinity of $\zeta=1$, as labeled by the ellipse. This irregularity can ultimately be attributed to a slight deviation of estimated ω_8 from the exact value. The abnormality of the profile of $Y(\omega)$ versus ω around ω_8 coincides with the irregularity of the 8^{th} mode shape, demonstrating the 8^{th}-mode bottleneck problem in solving its governing differential equations to acquire high-order modes of Mode I.

In essence, this bottleneck problem is attributed to the immense complexity of the transcendental frequency equation $D(\omega)=0$. That being the case, this type of bottleneck problem is a basic characteristic of stepped Timoshenko beams.

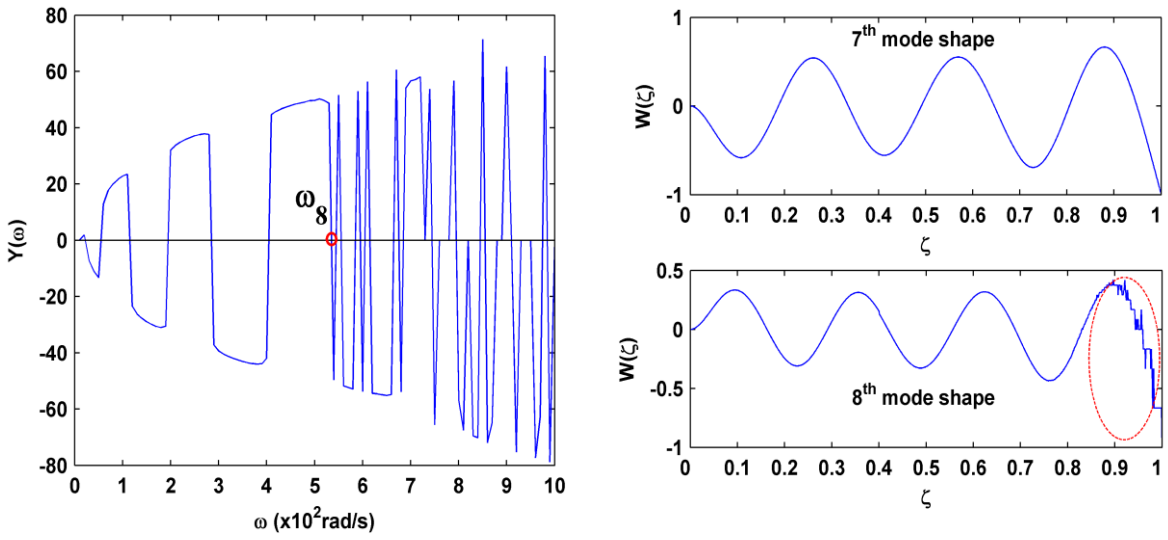

(a) (b)

Figure 3. 8th-mode bottleneck in acquisition of high-order modes by solving two-step Timoshenko beam frequency equation (Model 1). (a) Profile of frequency determinant $D(\omega)$ versus frequency ω; (b) 11th and 12th mode shapes.

2.3 Root cause analysis

The root cause of the bottleneck problem in solving governing differential equations to acquire high-order modes of stepped Timoshenko beam lies in the conflict between the huge capacity demand in evaluating the frequency determinant and the limited capacity of a digital computer.

As per equations (7)-(10), the hyperbolic functions $\sinh a_i$ and $\cosh a_i$, a_i increasing with ω, are two essential constituent components of the terms of the frequency equation $D(\omega)=0$. Each term of the frequency equation is constituted by multiple multiplied elements of $\sinh a_i$ and/or $\cosh a_i$. Among all the terms, the particular term consisting of the highest-order product of hyperbolic functions is called the dominant-term. In view of either $\sinh a_i$ or $\cosh a_i$ being an exponentially-increasing unbounded function, the dominant-term has the greatest possibility of arriving quickly at infinity with the increase of a_i (ω), posing

an immense capacity requirement for digital computers to properly process such a term.

Moreover, a digital computer has a limit to the precision of floating-point representation for a numerical quantity. For a common double-precision binary floating-point computer, that limit is 2^{53}, determined by the maximum significance digit according to the standard (IEEE, 2008). If the dominant-term exceeds 2^{53}, round-off errors in floating-point math occur. That being the case, the critical value 2^{53} of the dominant-term determines the upper bound of variable a_i in $\sinh a_i$ and $\cosh a_i$, in turn specifying the upper bound of variable ω, notated by ω_r. On the other hand, once ω exceeds ω_r, round-off errors occur, and the profile of $Y(\omega)$ versus ω behaves unreasonably, provoking the bottleneck problems as illustrated in Figure 3, so that ω is confined to a bounded frequency range.

The above analysis identifies the root cause of the bottleneck problems in acquiring high-order modes of a stepped Timoshenko beam by solving its governing differential equations.

3 Problem-solving method

3.1 LCS method

A LCS-based method (LCS method) is created to tackle the bottleneck problem. The LCS method uses a set of LCSs in place of GCS to provide alternative mathematical characterization of transverse vibration of a stepped Timoshenko beam. Use of this method to describe transverse vibration is illustrated on the preceding two-step Timoshenko beam (Figure 1): three LCSs (x_1,u_1), (x_2,u_2), and (x_3,u_3) (Figure 4) are introduced as an alternative to the GCS (x,w) as shown in Figure 1. In the *i*th LCS, the length of each segment is identified by the abscissa value S_i, which is related to the abscissa value L_i in the GCS by

$$S_i = L_i - L_{i-1}, \quad i = 1,2,3. \tag{12}$$

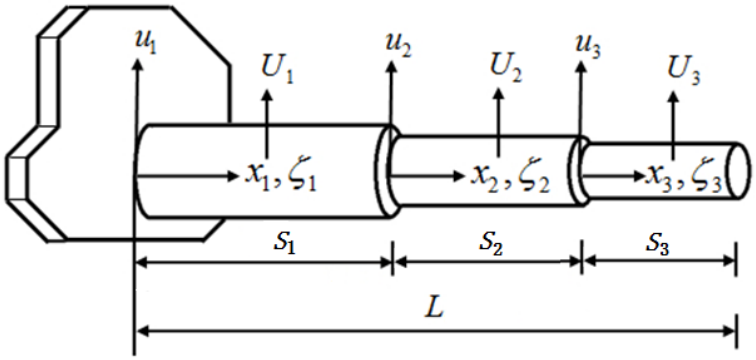

Figure 4. Two-step cantilever beam in LCS.

Within the LCSs, the transverse vibration of the *i*th segment of beam can be expressed by

$$E_i I_i \frac{\partial^2 v_i(x_i,t)}{\partial x_i^{\,2}} + k_i G_i A_i \left(\frac{\partial u_i(x_i,t)}{\partial x_i} - v_i(x_i,t) \right) - \rho_i I_i \frac{\partial^2 v_i(x_i,t)}{\partial t^2} = 0, \quad 0 \le x_i \le S_i, \tag{13.1}$$

$$k_i G_i \left(\frac{\partial^2 u_i(x_i,t)}{\partial x_i^{\,2}} - \frac{\partial v_i(x_i,t)}{\partial x_i} \right) - \rho_i \frac{\partial^2 u_i(x_i,t)}{\partial t^2} = 0, \quad 0 \le x_i \le S_i, \tag{13.2}$$

where the local coordinate x_i is related to the global coordinate x by $x_i = x - L_{i-1}$. Like $\zeta = x/L$, x_i is dimensionalized by $\eta_i = x_i/L$. Using the separation-of-variable method, the solutions of equations (13.1) and (13.2) can be represented by

$$u_i(x_i,t) = L U_i(x_i) e^{j\omega t}, \quad v_i(x_i,t) = V_i(x_i) e^{j\omega t}. \tag{14}$$

where U_i and V_i are the spatial solutions for the transverse deflection and rotational angle, respectively.

As the transverse vibration of every point in a beam is physically unique and independent of coordinate systems, the spatial solutions derived by the GCS and LCSs are identical:

$$W_i(\zeta) = U_i(\eta_i), \quad \psi_i(\zeta) = V_i(\eta_i). \tag{15}$$

Using equation (14), equation (3) can be converted into:

$$\frac{d^4}{d\eta_i^{\,4}} U_i(\eta_i) + 2\alpha_i \frac{d^2}{d\eta_i^{\,2}} U_i(\eta_i) + \beta_i U_i(\eta_i) = 0, \tag{16.1}$$

$$\frac{d^4}{d\eta_i^4}V_i(\eta_i)+2\alpha_i\frac{d^2}{d\eta_i^2}V_i(\eta_i)+\beta_i V_i(\eta_i)=0. \tag{16.2}$$

The general solutions for equation (16) can be expressed as

$$U_i(\eta_i)=A_i^*\cosh\gamma_{i,1}\eta_i+B_i^*\sinh\gamma_{i,1}\eta_i+C_i^*\cos\gamma_{i,2}\eta_i+D_i^*\sin\gamma_{i,2}\eta_i, \tag{17.1}$$

$$V_i(\eta_i)=A_i^*m_{i,1}\sinh\gamma_{i,1}\eta_i+B_i^*m_{i,1}\cosh\gamma_{i,1}\eta_i+C_i^*m_{i,2}\sin\gamma_{i,2}\eta_i-D_i^*m_{i,2}\cos\gamma_{i,2}\eta_i. \tag{17.2}$$

Using $\zeta_i=x_i/S_i$, $\gamma_{i,1}^*=\gamma_{i,1}S_i/L$, $\gamma_{i,2}^*=\gamma_{i,2}S_i/L$, $U_i(\eta_i)$ and $V_i(\eta_i)$ can be further represented in the local coordinate system:

$$U_i(\zeta_i)=A_i^*\cosh\gamma_{i,1}^*\zeta_i+B_i^*\sinh\gamma_{i,1}^*\zeta_i+C_i^*\cos\gamma_{i,2}^*\zeta_i+D_i^*\sin\gamma_{i,2}^*\zeta_i,\ 0\le\zeta_i\le1, \tag{18.1}$$

$$V_i(\zeta_i)=A_i^*m_{i,1}\sinh\gamma_{i,1}^*\zeta_i+B_i^*m_{i,1}\cosh\gamma_{i,1}^*\zeta_i+C_i^*m_{i,2}\sin\gamma_{i,2}^*\zeta_i-D_i^*m_{i,2}\cos\gamma_{i,2}^*\zeta_i,\ 0\le\zeta_i\le1. \tag{18.2}$$

and their derivatives $U_i^{'}(\zeta_i)$ and $V_i^{'}(\zeta_i)$ are

$$U_i^{'}(\zeta_i)=A_i^*\gamma_{i,1}\sinh\gamma_{i,1}^*\zeta_i+B_i^*\gamma_{i,1}\cosh\gamma_{i,1}^*\zeta_i-C_i^*\gamma_{i,2}\sin\gamma_{i,2}^*\zeta_i+D_i^*\gamma_{i,2}\cos\gamma_{i,2}^*\zeta_i,\ 0\le\zeta_i\le1, \tag{18.3}$$

$$V_i^{'}(\zeta_i)=A_i^*m_{i,1}\gamma_{i,1}\cosh\gamma_{i,1}^*\zeta_i+B_i^*m_{i,1}\gamma_{i,1}\sinh\gamma_{i,1}^*\zeta_i+C_i^*m_{i,2}\gamma_{i,2}\cos\gamma_{i,2}^*\zeta_i+D_i^*m_{i,2}\gamma_{i,2}\sin\gamma_{i,2}^*\zeta_i,\ 0\le\zeta_i\le1, \tag{18.4}$$

where $A_i^*-D_i^*, i=1,2,3$, are constants to be determined by the continuity and boundary conditions. The continuity conditions of the displacement, slope, moment, and shear force at the junctions of adjacent beam segments are

$$\begin{aligned}&U_i(\zeta_i)\big|_{\zeta_i=1}=U_{i+1}(\zeta_{i+1})\big|_{\zeta_{i+1}=0}, \qquad V_i(\zeta_i)\big|_{\zeta_i=1}=V_{i+1}(\zeta_{i+1})\big|_{\zeta_{i+1}=0},\\ &E_iI_iV_i^{'}(\zeta_i)\big|_{\zeta_i=1}=E_{i+1}I_{i+1}V_{i+1}^{'}(\zeta_{i+1})\big|_{\zeta_{i+1}=0}, \quad k_iG_iA_i(U_i^{'}(\zeta_i)-V_i(\zeta_i))\big|_{\zeta_i=1}=k_{i+1}G_{i+1}A_{i+1}(U_{i+1}^{'}(\zeta_{i+1})-V_{i+1}(\zeta_{i+1}))\big|_{\zeta_{i+1}=0},\end{aligned} \tag{19}$$

and the boundary conditions at the ends of the entire beam are

$$U_1(\zeta_1)\big|_{\zeta_1=0}=0, \quad V_1(\zeta_1)\big|_{\zeta_1=0}=0, \quad V_3^{'}(\zeta_3)\big|_{\zeta_3=1}=0, \quad (U_3^{'}(\zeta_3)-V_3(\zeta_3))\big|_{\zeta_3=1}=0. \tag{20}$$

Substituting equation (18) into equations (19) and (20) yields a linear algebraic homogeneous system

$$\mathbf{D}^*(\omega)\mathbf{C}^* = 0. \tag{21}$$

where superscript * indicates quantities for LCSs, similarly hereinafter. The frequency determinant $D^*(\omega)$ of the characteristic matrix D^* is

$$D^*(\omega) = \begin{vmatrix} O_{1(2\times4)}^* & 0_{(2\times4)} & 0_{(2\times4)} \\ P_{1(4\times4)}^* & Q_{1(4\times4)}^* & 0_{(4\times4)} \\ 0_{(4\times4)} & P_{2(4\times4)}^* & Q_{2(4\times4)}^* \\ 0_{(2\times4)} & 0_{(2\times4)} & O_{2(2\times4)}^* \end{vmatrix}, \tag{22}$$

with the non-zero sub-blocks O_1^*, O_2^*, P_1^*, P_2^*, Q_1^*, and Q_2^* given by

$$O_1^* = \begin{pmatrix} 1 & 0 & 1 & 0 \\ 0 & m_{1,1} & 0 & -m_{1,2} \end{pmatrix},$$

$$P_1^* = \begin{pmatrix} \cosh\gamma_{1,1}^* & \sinh\gamma_{1,1}^* & \cos\gamma_{1,2}^* & \sin\gamma_{1,2}^* \\ \gamma_{1,1}\sinh\gamma_{1,1}^* & \gamma_{1,1}\cosh\gamma_{1,1}^* & -\gamma_{1,2}\sin\gamma_{1,2}^* & \gamma_{1,2}\cos\gamma_{1,2}^* \\ m_{1,1}\gamma_{1,1}\cosh\gamma_{1,1}^* & m_{1,1}\gamma_{1,1}\sinh\gamma_{1,1}^* & m_{1,2}\gamma_{1,2}\cos\gamma_{1,2}^* & m_{1,2}\gamma_{1,2}\sin\gamma_{1,2}^* \\ (\gamma_{1,1}-m_{1,1})\sinh\gamma_{1,1}^* & (\gamma_{1,1}-m_{1,1})\cosh\gamma_{1,1}^* & -(\gamma_{1,2}+m_{1,2})\sin\gamma_{2,1}^* & (\gamma_{1,2}+m_{1,2})\cos\gamma_{1,2}^* \end{pmatrix},$$

$$Q_1^* = \begin{pmatrix} -1 & 0 & -1 & 0 \\ 0 & -\gamma_{2,1} & 0 & \gamma_{2,2} \\ -F_1 m_{2,1}\gamma_{2,1} & 0 & -F_1 m_{2,2}\gamma_{2,2} & 0 \\ 0 & -K_1(\gamma_{2,1}-m_{2,1}) & 0 & -K_1(\gamma_{2,2}+m_{2,2}) \end{pmatrix},$$

$$P_2^* = \begin{pmatrix} \cosh\gamma_{2,1}^* & \sinh\gamma_{2,1}^* & \cos\gamma_{2,2}^* & \sin\gamma_{2,2}^* \\ \gamma_{2,1}\sinh\gamma_{2,1}^* & \gamma_{2,1}\cosh\gamma_{2,1}^* & \gamma_{2,2}\sin\gamma_{2,2}^* & -\gamma_{2,2}\cos\gamma_{2,2}^* \\ m_{2,1}\gamma_{2,1}\cosh\gamma_{2,1}^* & m_{2,1}\gamma_{2,1}\sinh\gamma_{2,1}^* & m_{2,2}\gamma_{2,2}\cos\gamma_{2,2}^* & m_{2,2}\gamma_{2,2}\sin\gamma_{2,2}^* \\ (\gamma_{2,1}-m_{2,1})\sinh\gamma_{2,1}^* & (\gamma_{2,1}-m_{2,1})\cosh\gamma_{2,1}^* & -(\gamma_{2,2}+m_{2,2})\sin\gamma_{2,2}^* & (\gamma_{2,2}+m_{2,2})\cos\gamma_{2,2}^* \end{pmatrix},$$

$$Q_2^* = \begin{pmatrix} -1 & 0 & -1 & 0 \\ 0 & -\gamma_{3,1} & 0 & -\gamma_{3,2} \\ -F_2 m_{3,1}\gamma_{3,1} & 0 & -F_2 m_{3,2}\gamma_{3,2} & 0 \\ 0 & -K_2(\gamma_{3,1}-m_{3,1}) & 0 & -K_2(\gamma_{3,2}+m_{3,2}) \end{pmatrix},$$

$$O_2^* = \begin{pmatrix} m_{3,1}\gamma_{3,1}\cosh\gamma_{3,1}^* & m_{3,1}\gamma_{3,1}\sinh\gamma_{3,1}^* & m_{3,2}\gamma_{3,2}\cos\gamma_{3,2}^* & m_{3,2}\gamma_{3,2}\sin\gamma_{3,2}^* \\ (\gamma_{3,1}-m_{3,1})\sinh\gamma_{3,1}^* & (\gamma_{3,1}-m_{3,1})\cosh\gamma_{3,1}^* & -(\gamma_{3,2}+m_{3,2})\sin\gamma_{3,2}^* & (\gamma_{3,2}+m_{3,2})\cos\gamma_{3,2}^* \end{pmatrix}.$$

Setting the frequency determinant to zero yields the frequency equation:

$$D^*(\omega) = 0. \tag{23}$$

Solving equation (23) can produce a series of modal frequencies ω_j. Provided with ω_j, the coefficient vector $\mathbf{C}^*$ in equation (21) can be derived. Substituting ω_j and $\mathbf{C}^*$ into equations (18), the mode shape U_i^j can be obtained.

3.2. Features of $D^*(\omega)$

The LCS method endows the frequency determinant $D^*(\omega)$ with two distinctive features: a simplified structure and lower magnitude for entries in $D^*(\omega)$.

(1) Simplified structure

Notably, the representation of continuity conditions in LCSs (equation (19) is significantly different from that in a GCS (equation (5). Compared to equation (5), equation (19) contains more elements specified by the local abscissa as zero. These elements induce more occurrences of zero or unity for $\sinh\gamma_{i,1}^*$, $\sinh\gamma_{i,2}^*$, $\cosh\gamma_{i,1}^*$, and $\cosh\gamma_{i,2}^*$, causing the Q_1^* and Q_2^* of $D^*(\omega)$ to be constant sub-blocks, notated by $\mathbf{X_1}$ and $\mathbf{X_2}$. As shown in equation (24), $\mathbf{X_1}$ and $\mathbf{X_2}$ can largely reduce the dimensionality of $D^*(\omega)$, lower than that of $D(\omega)$ in the GCS with the counterparts of Q_1 and Q_2 containing numerous instances of $\sinh a_i$ and $\cosh a_i$. Clearly, $\mathbf{X_1}$ and $\mathbf{X_2}$ evoke a simpler dominant-term of frequency equation $D^*(\omega)$=0, allowing a greater ω_T to be determined by the limit capability (2^{53}) of a double-precision binary floating-point computer.

$$D^*(\omega)=\begin{vmatrix} O^*_{1(2\times4)} & 0_{(2\times4)} & 0_{(2\times4)} \\ P^*_{1(4\times4)} & \mathbf{X}_{1(4\times4)} & 0_{(4\times4)} \\ 0_{(4\times4)} & P^*_{2(4\times4)} & \mathbf{X}_{2(4\times4)} \\ 0_{(2\times4)} & 0_{(2\times4)} & O^*_{2(2\times4)} \end{vmatrix}. \tag{24}$$

(2) Lower magnitude for elements in $D^*(\omega)$

Aside from the simplified structure, the magnitude of the any hyperbolic function in $D^*(\omega)$ is lower than or equal to that of its counterpart in $D(\omega)$. This feature can be attributed to the facts that:

$$\gamma^*_{i,1}=\gamma_{i,1}\frac{S_i}{L}\le\gamma_{i,1}\frac{L_i}{L}=\gamma_{i,1}l_i,\quad \gamma^*_{i,2}=\gamma_{i,2}\frac{S_i}{L}\le\gamma_{i,2}\frac{L_i}{L}=\gamma_{i,2}l_i, \tag{25}$$

caused by $S_1=L_1$, $S_2<L_2$, $S_3<L_3$.

Equation (25) draws on the relations between the corresponding elements in $D^*(\omega)$ and $D(\omega)$: $\sinh(\gamma^*_{i,1})\le\sinh(\gamma_{i,1}l_i)$ and $\cosh(\gamma^*_{i,1})\le\cosh(\gamma_{i,1}l_i)$, resulting in the top-term of $D^*(\omega)$ being remote from the critical value 2^{53}, thus realizing greater ω_T.

The above two features of $D^*(\omega)$ produced by the LCSs lead to a frequency equation of reduced complexity, conducive to acquisition of high-order mode shapes of a stepped Timoshenko beam.

4 Performance evaluation

4.1 Comparison of LCS and GCS methods

(1) Model I

For brevity, the conventional GCS-based method to calculate high-order modes is termed the GCS method. Use of the LCS method to evaluate modes of a two-step Timoshenko beam is

demonstrated using Model I (Table 1 and Table 2). To present a wider frequency scope, the profile of $Y^*(\omega)$ (the superscript * labels the LCS method) versus ω replaces the profile of $D^*(\omega)$ versus ω, as per equation (11). From the profile of $Y^*(\omega)$ versus ω (Figure 5), the first 33 modal frequencies can be properly determined, far beyond the first 8 modal frequencies identified by the profile of $Y(\omega)$ versus ω (Figure 3(a)) from the GCS method. Therefore, the proposed LCS method largely overcomes the 8th-mode bottleneck for a two-step Timoshenko beam.

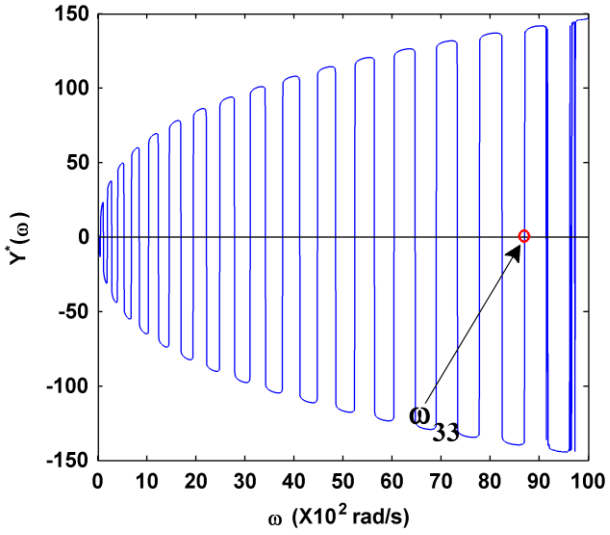

Figure 5. Profile of $Y^*(\omega)$ versus ω from the LCS method for Model I.

(2) Models II-IV

Acquisition of high-order modes for Models II-IV (Table 1 and Table 2) with more steps are further conducted for comprehensively assessing the performance of the LCS method. First, the profiles of $Y(\omega)$ versus ω for Models II-IV are yielded by the GCS method, as shown in Figures 6 (a), 6(c), and 6(e), respectively. In the figure, only the first 5, 6, and 4 modal frequencies are identified, illustrating bottlenecks in the acquisition of higher-order modes of Models II-IV, respectively. In contrast, the profiles of $Y^*(\omega)$ versus ω resulting from the

LCS method, shown in Figures 6(b), 6(d), and 6(f), allow determination of the first 44, 67, and 42 modal frequencies for Models II-IV, respectively. Comparing the pairs of Figures. 6(a) and 6(b), 6(c) and 6(d), and 6(e) and 6(f), one can conclude the LCS method effectively circumvents the bottlenecks in the acquisition of higher-order modes of stepped Timoshenko beams.

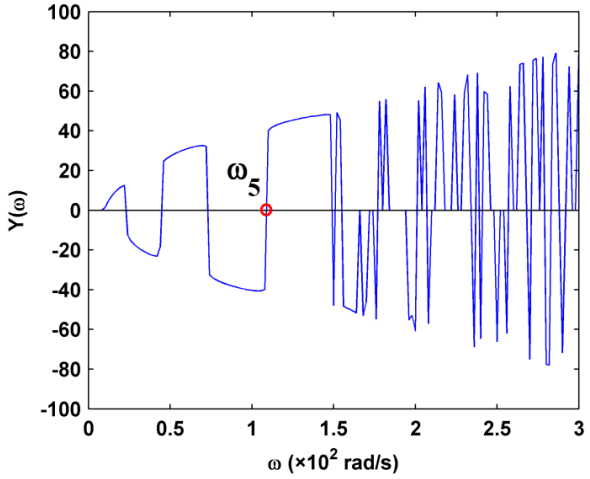

(a)

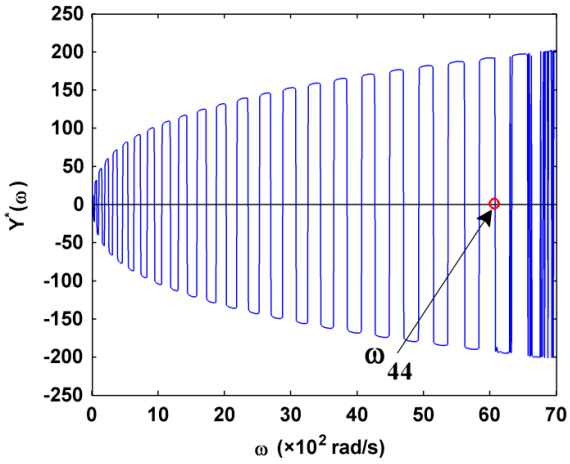

(b)

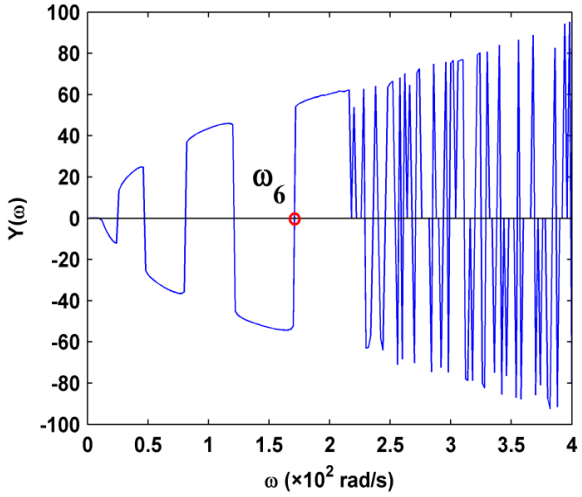

(c)

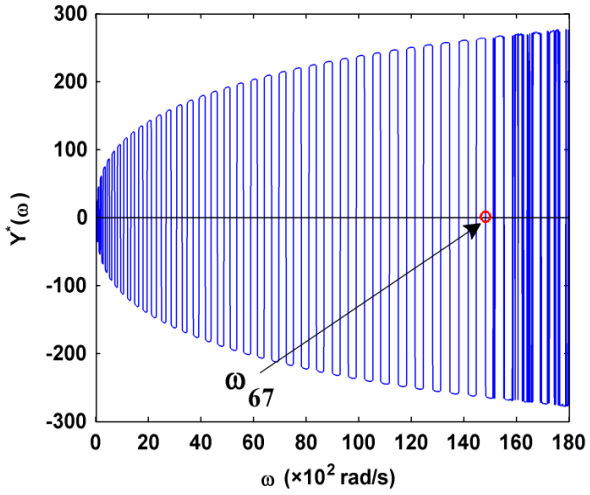

(d)

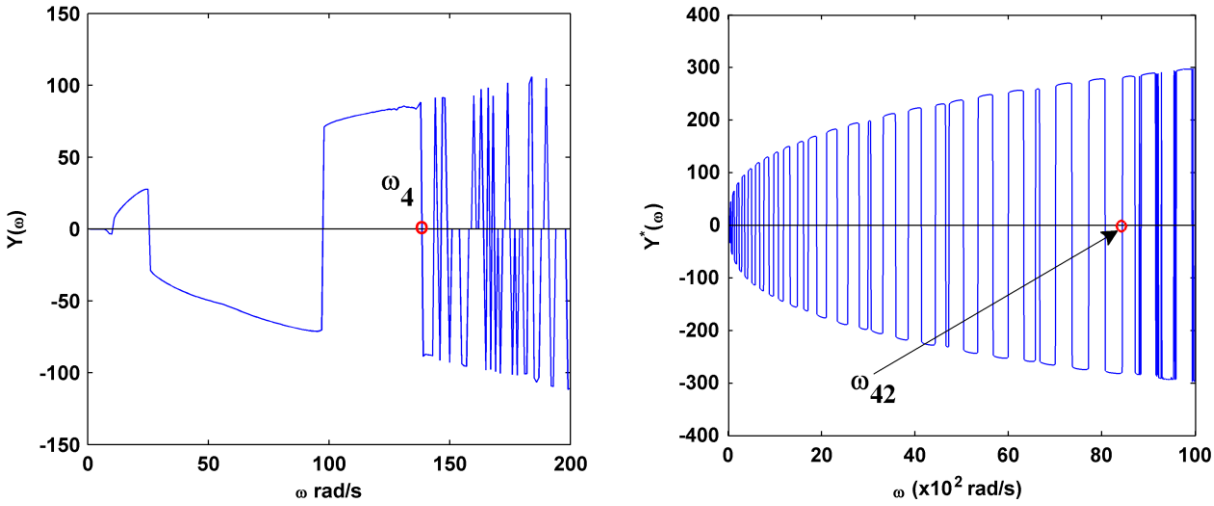

(e) (f)

Figure 6. Profiles of (a), (b), and (c) $Y(\omega)$ versus ω and (a), (b), and (c) $Y^*(\omega)$ versus ω (Models II-IV) yielded by the GCS method and the LCS method, respectively.

4.2 Comparison of LCS and EDS methods

The accuracy, capacity, and efficiency of the LCS method in acquiring high-order modes of a stepped Timoshenko beam are assessed using the well-known EDS scheme involving the W-W algorithm as a reference. As widely demonstrated (Howson and Williams, 1973; Pilkey and Kitis, 1994; Banerjee and Williams, 1996; Banerjee, 1997; Banerjee, 2001; Banerjee, 2003; Yuan et al., 2007; Li et al., 2008; Yu and Roesset, 2011; Greco and Pau, 2012), the EDS scheme is a valid method to achieve high-order modes of a stepped Timoshenko beam, with no need for solving the governing differential equations of the beam.

4.2.1 Accuracy

The accuracy comparison between the LCS method and the EDS scheme is illustrated on Model I with the results shown in Table 3. With the EDS scheme (Yu and Roesset, 2011), each beam segment of Model I is regarded as a Timoshenko beam member of 4 degrees of freedom (two pairs of displacement and rotation angle at two ends), from which the member's EDS matrix is formulated with the frequency-dependent exact shape functions. The EDS matrices of three members are assembled to form a global EDS matrix, on which the W-W algorithm runs

to yield all possible modal frequencies. The portion of modal frequencies is labeled by 'EDS' in Table 3, in which the 'GCS' and 'LCS' designate the modal frequencies obtained by the GCS and LCS methods. Clearly, the first 8 modal frequencies – within the capacity of the GCS method – are almost identical for GCS, LCS, and EDS methods; the modal frequencies up to the 33th order – within the capacity of the LCS method – are approximately identical for the LCS and EDS methods, with the maximum relative error ε <0.1%. These small errors can be attributed to the extensive use of matrix manipulations in GCS, LCS, and EDS, undertaken by a digital computer of limited precision (Erdelyi and Hashemi, 2012). For the LCS and EDS methods, almost identical accuracy can be easily found for other types of stepped Timoshenko beams, e.g., Modes II-IV.

Table 3. Modal frequencies for Model I obtained by GCS and LCS methods

Mode	GCS (ω [rad/s])	LCS (ω [rad/s])	EDS (ω [rad/s])	Relative error (ε [%])
1	4.214	4.214	4.214	0.000
2	22.980	22.980	22.979	0.004
3	59.400	59.400	59.400	0.000
4	117.594	117.594	117.601	0.006
5	193.426	193.426	193.413	0.007
6	287.277	287.276	287.246	0.010
7	400.996	400.990	400.900	0.022
8		533.675	533.669	0.001
9		684.500	684.366	0.020
10		846.888	846.888	0.000
11		1037.264	1037.383	0.011
12		1239.232	1238.957	0.022
13		1452.708	1452.474	0.016
14		1692.380	1692.702	0.019
15		1943.103	1942.860	0.013
16		2210.113	2209.411	0.032
17		2486.542	2486.800	0.010
18		2789.415	2789.658	0.009
19		3101.337	3100.157	0.038
20		3415.482	3415.061	0.012
21		3763.157	3761.347	0.048
22		4112.409	4111.233	0.029
23		4472.721	4471.087	0.037
24		4846.579	4847.700	0.023
25		5237.976	5237.871	0.002
26		5638.697	5635.894	0.050
27		6034.027	6033.886	0.002
28		6465.979	6467.858	0.029
29		6894.382	6891.348	0.044

30	7324.726	7322.197	0.035
31	7778.345	7779.690	0.017
32	8232.764	8233.985	0.015
33	8699.980	8698.093	0.022

4.2.2 Capacity

The capacity comparison between the LCS method and the EDS scheme is illustrated on Model V with the results shown in Figure 7 and Table 4. The EDS scheme is capable of achieving almost all solutions to high-order modes of a stepped Timoshenko beam. In contrast to this scheme, the LCS method exploits the LCSs to simplify frequency equation to accomplish higher-order modes. The LCS method can easily increase of its capacity to accommodate and acquire high-order modes by a strategy of pseudo step. A pseudo step is defines as a virtual step that divides a uniform beam into two sub-segments. The introduction of a pseudo step can increase the number of LCSs and therefore induce greater simplification of the frequency equation, offering larger capacity of accomplishing high-order modes.

Model V is produced by introducing a pseudo step into the first beam segment of Model I to form two sub-segments. The vibration of each sub-segment is accounted for by a new LCS. Collectively, a set of four LCSs are responsible for the vibration of all four beam segments of Model V. The obtained profile of $Y^*(\omega)$ versus ω is shown in Figure 7, where the first 54 modal frequencies are properly determined within the frequency range up to 20,000 Hz. Table 4 presents the modal frequencies up to the 54th order by saving the first 33 modal frequencies (Table 3). In the table, the LCS and the EDS scheme agree with each other well, with the maximum relative error ε <0.1%. Clearly, the strategy of pseudo step can significantly increase the capacity of the LCS method to approach high-order modes. With introducing more pseudo steps, the increasingly-sized LCSs can arrive at any high-order modes of interest. Therefore, the LCS method involving pseudo steps provides a tactical strategy to acquire high-order modes of a stepped Timoshenko beam.

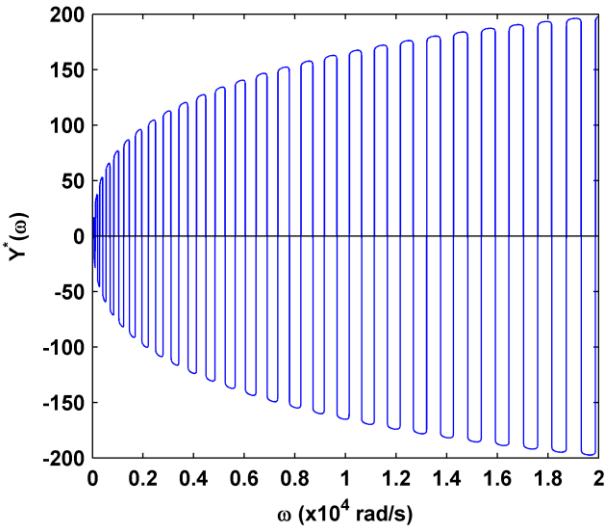

Figure 7. Profile of $Y^*(\omega)$ versus ω (Model V) yielded by LCS method with one pseudo step.

Table 4. Modal frequencies for Model V obtained by LCS method and EDS scheme

Mode	LCS (ω [rad/s])	EDS (ω [rad/s])	Relative error ε (ε [%])
34	9162.653	9163.556	0.010
35	9656.310	9658.415	0.022
36	10146.172	10140.508	0.056
37	10627.394	10624.400	0.028
38	11139.600	11144.050	0.040
39	11648.083	11644.572	0.030
40	12163.248	12156.238	0.058
41	12673.578	12676.329	0.022
42	13210.344	13212.052	0.013
43	13746.828	13738.067	0.064
44	14265.016	14262.225	0.020
45	14820.597	14826.813	0.042
46	15367.464	15361.033	0.042
47	15914.721	15905.737	0.057
48	16464.437	16469.361	0.030
49	17031.078	17031.534	0.003
50	17601.578	17589.508	0.069
51	18147.373	18145.468	0.010
52	18732.907	18740.361	0.040
53	19309.500	19299.756	0.050
54	19879.000	19866.967	0.061

4.2.3 Efficiency

As evaluating high-order modes using the EDS scheme, the W-W algorithm plays a key role of finding modal frequencies by processing the global EDS matrix (Williams and Wittrick, 1970;

Wittrick and Williams, 1971; Williams and Wittrick, 1983; Williams and Kennedy, 2010; Howson and Williams, 1973; Pilkey and Kitis, 1994; Banerjee and Williams, 1996; Banerjee, 1997; Banerjee, 2001; Banerjee, 2003; Yuan et al., 2007; Li et al., 2008; Yu and Roesset, 2011; Greco and Pau, 2012). Compared with the W-W algorithm, the classical method, which solves the modal frequencies by vanishing the determinant of the global EDS matrix, would induce missing of roots (Howson and Zare, 2005). The W-W algorithm is essentially an indirect numerical method. This algorithm seizes a certain modal frequency based on calculating the number of modal frequencies that are below a given trial frequency value rather than directly evaluating the eigenvalues of the global EDS matrix. Aside from the generally stated merits such as great accuracy and strong reliability in capturing modal frequencies, the W-W algorithm can only address one modal frequency for one time, involving multiple iterations to converge on the modal frequency (Banerjee and Williams, 1996). That being the case, evaluation of a large range of modal frequencies up to a quite high order requires consecutive execution of the W-W algorithm as many times as the number of modal frequencies of interest, resulting in an impaired efficiency.

In contrast, the LCS method delivers high-order modal frequencies of a stepped Timoshenko beam by directly solving its governing differential equation. This mechanism renders the LCS method to produce all the modal frequencies of interest at a time as long as the pseudo steps are enough. Specifically, the zero-crossings of the profile of $Y^*(\omega)$ versus ω simultaneously specify the modal frequencies, as displayed in Figure and 7. Moreover, the frequency determinant from the characteristic matrix for the LCS method commonly enjoys a super regularity to that from the global EDS matrix for the EDS scheme. The frequency determinant from the global EDS matrix (Model I) is illustrated in Figure 8, which is interior to the frequency determinant from the characteristic matrix for the LCS method, shown in Figure 5. Therefore, the lower regularity in Figure 8 offers more possibility of causing false roots and missing roots of modal frequency (Howson and Zare, 2005). With the super regularity of frequency determinant, the LCS method has higher operational efficiency than the EDS

scheme in accomplishing high-order modes of interest.

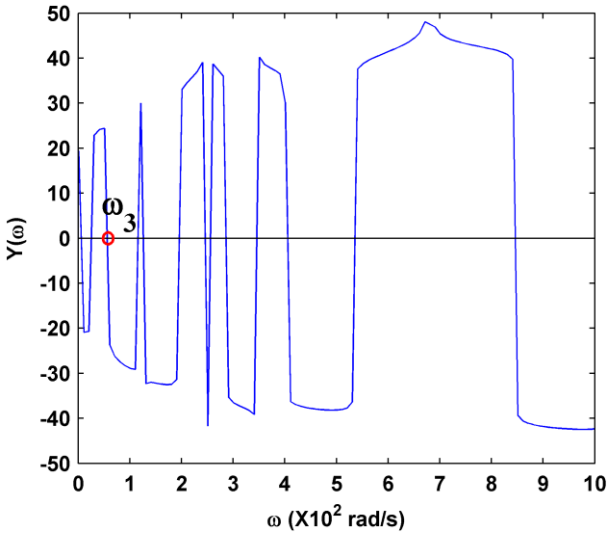

Figure 8. Frequency determinant (Model I) from the global EDS matrix for the EDS scheme.

5 Conclusions

This study develops a new method to acquire the high-order modes of a stepped Timoshenko beam by solving its governing differential equations. The method exploits a set of LCSs in place of the conventional single GCS to reformat the governing differential equations of a stepped Timoshenko beam. The frequency equation arising from the reformatted governing differential equations can be significantly simplified by the LCSs, providing an opportunity of calculating high-order modal frequencies. The accuracy, capacity, and efficiency of the LCS method are corroborated by using the well-known EDS scheme involving the W-W algorithm as a reference. Differing from the EDS scheme that follows the idea of FE method to obtain the solutions to high-order modes, the LCS method attains high-order modes by solving the governing differential equations of a stepped Timoshenko beam.

Acknowledgments

M. Cao is grateful to the partial support provided by the Natural Science Foundations of China

(No. 11172091), Qing Lan Project and the Fundamental Research Funds for the Central Universities (Grant Nos. 2014B03914 and 2012B05814).

References

Banerjee JR and Williams FW (1996) Exact dynamic stiffness matric for composite Timoshenko beams with applications. *Journal of Sound and Vibration* 194(4): 573-585.

Banerjee JR (1997) Dynamic stiffness formulation for structural elements: a general approach. *Computers and Structures* 63(1): 101-103.

Banerjee JR (2001) Dynamic stiffness formulation and free vibration analysis of centrifugally stiffened Timoshenko beams. *Journal of Sound and Vibration* 247(1): 97-115.

Banerjee JR (2003) Free vibration of sandwich beams using the dynamic stiffness method. *Computers and Structures* 81: 1915- 1922.

Caliò I and Greco A (2012) Free vibrations of Timoshenko beam-columns on Pasternak foundations. *Journal of Vibration and Control* 19(5): 686-696.

Dawe DJ (1978) A finite element for the vibration analysis of Timoshenko beams. *Journal of Sound and Vibration* 60(1): 11-20.

Dong XJ, Meng G, Li HG and Ye L (2005) Vibration analysis of a stepped laminated composite Timoshenko beam. *Mechanics Research Communications* 32: 572-581.

Erdelyi NH and Hashemi SM (2012) A dynamic stiffness element for free vibration analysis of delaminated layered beams. *Modelling and Simulation in Engineering* 2012: 492415.

Failla G (2011) Closed-form solutions for Euler-Bernoulli arbitrary discontinuous beams. *Archive of Applied Mechanics* 81: 605-628.

Goncalves PJP, Brennan MJ and Elliott SJ (2007) Numerical evaluation of high-order modes of vibration in uniform Euler-Bernoulli beams. *Journal of Sound and Vibration* 301: 1035-1039.

Greco A and Pau A (2012) Damage identification in Euler frames. *Computers and Structures* 92-93: 328- 336.

Gupta AP and Sharma N (1998) Effect of transverse shear and rotator inertia on the forced motion of a stepped rectangular beam. *Journal of Sound and Vibration* 209(5): 811-820.

Han SM, Benaroya H and Wei T (1999) Dynamics of Transversely Vibrating Beams Using Four Engineering Theories. *Journal of Sound and Vibration* 225(5): 935-988.

Horr AM and Schmidt LC (1995) Closed-form solution for the Timoshenko beam theory using a computer-based mathematical package. *Computers and Structures* 55(3): 405-412.

Howson WP and Williams FW (1973) Natural frequencies of frames with axially loaded Timoshenko members. *Journal of Sound and Vibration* 26(4): 503-515.

Howson WP and Zare A (2005) Exact dynamic stiffness matrix for flexural vibration of three-layered sandwich beams. *Journal of Sound and Vibration* 282:753-767.

Hsu JC, Lee HL and Chang WJ (2007) Flexural vibration frequency of atomic force microscope cantilevers using the Timoshenko beam model. *Nanotechnology* 18: 285503.

Huang TC (1961) The effect of rotatory inertia and of shear deformation on the frequency and normal mode equations of uniform beams with simple end conditions. *Journal of Applied Mechanics* 28(4) (1961) 579-584.

Institute of Electrical and Electronics Engineers (2008) *754-2008-IEEE Standard for Floating-Point Arithmetic*. New York: IEEE.

Ju F, Lee HP and Lee KH (1994) On the free vibration of stepped beams. *International Journal of Solids and Structures* 31(22): 3125-3137.

Kapur KK (1966) Vibrations of a Timoshenko beam, using finite-element approach. *The Journal of the Acoustical Society of America* 40(5): 1058.

Khaji N, Shafiei M and Jalalpour M (2009) Closed-form solutions for crack detection problem of Timoshenko beams with various boundary conditions. *International Journal of Mechanical*

Sciences 51: 667-681.

Kisa M and Arif Gurel M (2007) Free vibration analysis of uniform and stepped cracked beams with circular cross sections. *International Journal of Engineering Science* 45: 364-380.

Lee CY, Zhuo HC and Hsu CW (2009) Lateral vibration of a composite stepped beam consisted of SMA helical spring based on equivalent Euler-Bernoulli beam theory. *Journal of Sound and Vibration* 324: 179-193.

Lee HP and Ng TY (1994) Vibration and buckling of a stepped beam. *Applied Acoustics* 42: 257-266.

Li J, Chen Y and Hua HX (2008) Exact dynamic stiffness matrix of a Timoshenko three-beam system. *International Journal of Mechanical Sciences* 50: 1023-1034.

Lin HP (2004) Direct and inverse methods on free vibration analysis of simply supported beams with a crack. *Engineering Structures* 26: 427-436.

Low KH (1993) A reliable algorithm for solving frequency equations involving transcendental functions. *Journal of Sound and Vibration* 161: 369-377.

Lu ZR, Huang M, Liu JK, Chen WH and Liao WY (2009) Vibration analysis of multiple-stepped beams with the composite element model. *Journal of Sound and Vibration* 322: 1070-1080.

Majkut L (2009) Free and forced vibrations of Timoshenko beams described by single difference equation. *Journal of Theoretical and Applied Mechanics* 47(1): 193-210.

Naguleswaran S (2002) Vibration of an Euler-Bernoulli beam on elastic end supports and with up to three step changes in cross-section. *International Journal of Mechanical Sciences* 44: 2541-2555.

Park JS and Stallings JM (2003) Lateral-torsional buckling of stepped beams. *Journal of Structural Engineering* 129: 1457-1465.

Park JS and Stallings JM (2005) Lateral-torsional buckling of stepped beams with continuous

bracing. *Journal of Bridge Engineering* 10: 87-95.

Pilkey WD and Kitis L (1994) Dynamic stiffness matrix for a beam element with shear deformation. *Shock and Vibration* 2(1): 155-162.

Suddoung K, Charoensuk J and Wattanasakulpong N (2013) Application of the differential transformation method to vibration analysis of stepped beams with elastically constrained ends. *Journal of Vibration and Control* 19(16): 2387-2400.

Tang Y (2003) Numerical evaluation of uniform beam modes. *Journal of Engineering Mechanics* 12: 1475-1477.

Timoshenko SP (1922) On the transverse vibrations of bars of uniform cross-section. *Philosophical Magazine* 43(253): 125-131.

Tong X, Tabarrok B and Yeh KY (1995) Vibration analysis of Timoshenko beams with non-homogeneity and varying cross-section. *Journal of Sound and Vibration* 186(5): 821-835.

Wei GW, Zhao YB and Xiang Y (2002) A novel approach for the analysis of high-frequency vibrations. *Journal of Sound and Vibration* 257(2): 207-246.

Williams FW and Wittrick WH (1970) An automatic computational procedure for calculating modal frequencies of skeletal structures. *International Journal of Mechanical and Sciences* 12(9):781-791.

Williams FW and Wittrick WH (1983) Exact buckling and frequency calculations surveyed. *Journal of Structural Engineering* 109(1): 169-187.

Williams FW and Kennedy D (2010) Historic, recent and ongoing applications of the Wittrick-Williams algorithm. *Computational Technology Reviews* 2:223-246.

Wittrick WH and Williams FW (1971) A general algorithm for computing modal frequencies of elastic structures. *The Quarterly Journal of Mechanics and Applied Mathematics* 24(3): 263-284.

Wu TX and Thompson DJ (1999) A double Timoshenko beam model for vertical vibration

analysis of railway track at high frequencies. *Journal of Sound and Vibration* 224(2): 329-348.

Xu W, Cao MS, Ren QW and Su ZQ (2014) Numerical evaluation of high-order modes for stepped beams. *Journal of Vibration and Acoustics* 136(1) 014503.

Yu CP and Roesset JM (2011) Dynamic stiffness matrices for linear members with distributed mass. *Tamkang Journal of Science and Engineering* 4(4): 253-264.

Yuan S, Ye KS, Xiao C, Williams FW and Kennedy W (2007) Exact dynamic stiffness method for non-uniform Timoshenko beam vibrations and Bernoulli-Euler column buckling. *Journal of Sound and Vibration* 303: 526-537.

Zhang ZG, Huang XC, Zhang ZY and Hua HX (2014) On the transverse vibration of Timoshenko double-beam systems coupled with various discontinuities. *International Journal of Mechanical Sciences* 89: 222-241.